

Random laser action in 3-D ZnO nanostructures

L. Miao^{1,2*}, S. Tanemura^{1,2}, H. Y. Yang³, S. P. Lau³, and G. Xu¹

¹ Key Laboratory of Renewable Energy and Gas Hydrate, Guangzhou Institute of Energy Conversion, Chinese Academy of Sciences, No. 2 Nengyuan Rd. Tianhe district, Guangzhou 510640, P.R. China

² Materials R & D Laboratory, Japan Fine Ceramics Centre, 2-4-1 Mutsuno, Atsuta-ku, Nagoya 456-8587, Japan

³ School of Electrical and Electronic Engineering, Nanyang Technological University, Block S2, Nanyang Avenue, 639798 Singapore

Received 29 July 2008, revised 30 November 2008, accepted 8 December 2008

Published online 17 April 2009

PACS 42.25.Dd, 42.55.Zz, 61.46.Km, 78.20.Ci, 78.67.Bf, 81.07.-b

* Corresponding author: e-mail miaolei@ms.giec.ac.cn, Phone: +86208703-5351, Fax: +86 20 8703-5351

Room-temperature ultraviolet random lasing with low threshold pumping power was successfully achieved by ZnO 3-D random-wall nanostructure fabricated on ZnO/SiO₂/Si substrate through a thermal chemical reaction and vapor transportation deposition method in a simple horizontal tube furnace from the mixed ZnO and graphite powders. The nanorods grown along c-axis on the substrate are coalesced to form the 3-D nano-wall with 80–100 nm in wall thickness and irregular height ranging of 95–250 nm. Mueller matrix spectroscopic ellipsometry reveals that evaluated refractive indices $n(E)$ of ZnO nanowalls are well interpreted by taking

account of the ratio between ZnO and void achieved by effective medium theory analysis and isotropic depolarization feature of the designated nanowalls. Random lasing action observed in the wide wavelength range between 375 and 395 nm is realized by coherent amplification of the closed-loop scattered light inside 3-D random-wall nanostructure. It is demonstrated that both transverse electric (TE) and transverse magnetic (TM) modes show the same threshold and pumping power dependent trend, while the intensity of TM lasing is weaker than that of TE due to the different scattering strength originated from the features of the inside of nano wall.

© 2009 WILEY-VCH Verlag GmbH & Co. KGaA, Weinheim

1 Introduction Nanostructured inorganic crystals with tunable morphologies are desirable for optimization in many potential applications in energy conversion, electronics, catalysis, optics, chemical sensing, and medical use. Zinc oxide (ZnO), a direct wide band gap (3.37 eV) semiconductor with a large excitation binding energy (60 meV), is one of the most important functional oxide, exhibiting near-UV emission [1], transparent conductivity, and piezoelectricity [2]. The growth of patterned and aligned one dimensional (1D) ZnO nanostructures is an interesting work, on the other hand, the growth of 2D and 3D nanostructures have also attracted much attention because of their interesting properties and potential to allow exploration of fundamental physical concepts and technological applications [3,4].

Ultraviolet (UV) light-emitting devices have diverse applications in scientific research [5, 6], medical apparatus [7, 8] and commercial products [9]. Hence, the realization

of UV light-emitting diodes (LEDs) and lasers, especially for the use of ZnO semiconductor, has been the focus of the recent researchers. Low threshold lasing of laser dye in a colloidal suspension of TiO₂ nanoparticles [10] has been theoretically and experimentally studied extensively. A random walking model has been widely accepted for this phenomenon [10–12]; therefore this isotropic low threshold laser emission is called “random laser.” The discovery of random lasing has stimulated many experimental and theoretical studies [13, 14] attracted by the possible application of this kind of micro-laser. However, no practical random laser has been fabricated as it is very difficult to process powders or solutions into devices [15].

Recently, Yu *et al.* demonstrated ZnO thin-film random lasers on silicon substrates using a simple thermal annealing technique [16–18]. Laser cavities, due to closed-looped optical scattering from the lateral facets of the irregular ZnO grains, were generated through post-growth

annealing of ZnO films. This approach has opened up a new way to construct random lasers on silicon.

Considering the complex fabrication process and film structure for obtaining random lasing in our previous works [19, 20], we proposed one simple method: thermal chemical reaction and vapor transport deposition technique in a tube furnace to fabricate low-cost and mass-production of ZnO 3-D random-wall nanostructure on ZnO/SiO₂/Si substrate without any catalyst and additives and observed lasing action at the wavelengths between 375 and 395 nm by the designated nanostructure under optical excitation by a frequency-tripled Nd:YAG laser (355 nm) at pulsed operation (6 ns pulse width, 10 Hz) as the world premier.

In this work, the fabrication conditions of the designated nanostructures were duplicated for preparation of the new series of the samples, the morphology of 3-D random-wall nanostructure was investigated in detail by scanning electron microscopy (SEM), random laser action in similar UV region and polarization effect of the emitting laser was tested, and finally refractive indices $n(E)$ (1.5–1.8 eV), depolarization effect and its incident angle dependency of the ZnO nanowall were evaluated by Mueller matrix spectroscopic ellipsometry (MMSE) respectively.

2 Experiment ZnO 3-D random-wall nanostructures were fabricated by a horizontal tube furnace system. The system consists of four main parts such as (i) a tube furnace, (ii) a horizontal quartz tube, (iii) a vacuum pump, and (iv) oxygen gas introduction system. ZnO nanostructures were synthesized on silicon substrate by the following steps: (i) thermally evaporated ZnO vapor is reduced into Zn or ZnO_x vapor by mixed graphite, (ii) then, Zn or ZnO_x vapor is oxidized into ZnO vapor by the introduced oxygen flow, and (iii) ZnO vapor is transported onto substrate by oxygen flow and being deposited on substrate to produce nano structures in the non-direct heating zone of the tube furnace. A buffer layer, with refractive index lower than that of the ZnO film, is needed between the ZnO film and Si substrate in order to achieve transverse confinement of light inside the ZnO nanostructure. In the present case, amorphous SiO₂ thin film was used.

We again emphasize the several key steps of the synthesis as: (i) growth of 300-nm-thick SiO₂ on Si substrate by thermal dry oxidation at 1000 °C for 3h; (ii) prior deposition of a 300-nm-thick ZnO thin film on substrate by helium rf magnetron sputtering, and finally (iii) growth of ZnO nanostructures in the quartz tube inserted in the tube furnace through the above described chemical processes.

Zinc oxide powders (high purity chemicals, 99.9%) and graphite powders (high purity chemicals, 99.9%) were mixed together, and being set in heating zone, while the substrate was placed in the bottom of the quartz tube in order to adjust the vapour transport direction. The parameters, such as: total pressure (P_{tot}), oxygen gas flow rate (GFR), deposition time (T_{dep}), powders heating temperature (T_p), substrate temperature (T_s), and the weight percentage between ZnO powder and carbon powder (C), were opti-

mized. The optimal experiment conditions for synthesis of ZnO 3-D nanostructure are summarized in Table 1.

Table 1 Optimal fabrication conditions for ZnO nanowalls.

| T_p/T_s (°C) | T_{dep} (min) | C=ZnO:C (mg) | P_{tot} (Pa) | GFR (ml/min) |
|-------------------|---------------------------|-----------------|--------------------------|-----------------|
| 1000/730 | 30 | 500:20 | 40 | 150 |

The morphology of nanostructure was observed by SEM. The crystal quality was evaluated by X-ray diffraction (XRD) and photoluminescence (PL). The random laser action of ZnO nanostructure was studied under optical excitation by a frequency-tripled Nd:YAG laser (355 nm) at pulsed operation (6 ns pulse width, 10 Hz). Optical pump was achieved by using a cylindrical lens to focus a pumping strip of 5 mm length and 60 μm width onto sample vertically. A polarizer was set before the detector in order to analyze the polarization state of lasing light. The TE (TM) polarization is defined as the direction parallel (perpendicular) to the sample substrate surface.

The refractive indices, isotropic depolarization effect and its incident angle dependency of ZnO 3-D random-wall were investigated by MMSE (MM-16, Horiba Jobin-Yvon Co.) in the wavelength range of 848–429 nm.

3 Results and discussion

3.1 SEM images

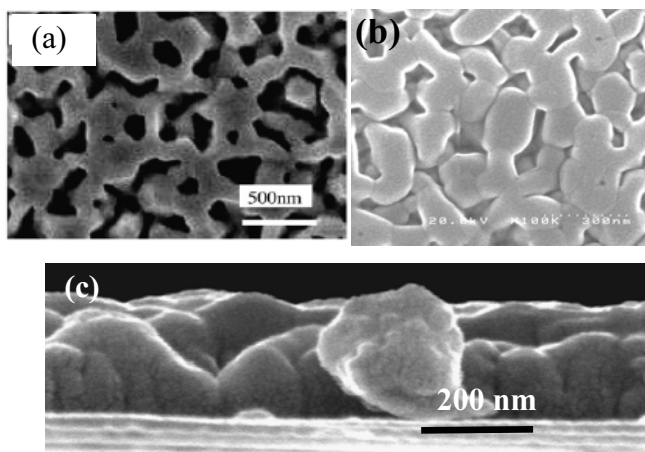


Figure 1 SEM images of 3-D ZnO nanowalls (a) surface view; (b) tilt view; (c) cross-sectional view.

Figure 1 shows the surface, tilt and cross-sectional SEM views of the fabricated 3-D ZnO nanowalls. No any isolated nanorod is observed in this structure, and the nanorods grown along c-axis are coalesced to form random wall with 80–100 nm in wall thickness. The surface and tilt views in Figs. 1(a) and (b) reveal that (i) the cavities have not regular shape, (ii) all of them are not vertically drilled through to ZnO buffer layer, and (iii) hexagonal facet still

can be observed in some areas. The wall has irregular height from 95-250 nm as shown in Fig. 1(c). We call this structure as “3-D random-wall nanostructure”.

3.2 Spectroscopic ellipsometry analysis and refractive index The Mueller matrix provides the most general and complete description of the response of a medium to excitation by polarized light in either reflection or transmission configurations. The Mueller matrix totally characterizes the optical properties of the sample by the interaction of a polarized light with mater in the absence of non-linear effects. The details of the MMSE analysis including of the employed film configuration model and the optical functions applied to respective films will be reported elsewhere. We emphasize that employed basic optical function to approximate refractive index $n(E)$ and $k(E)$ was 2-term Frouhi-Bloomer (F & B) dispersion formula [21, 22]. The thicknesses achieved by MMSE agree satisfactorily with that of SEM observation.

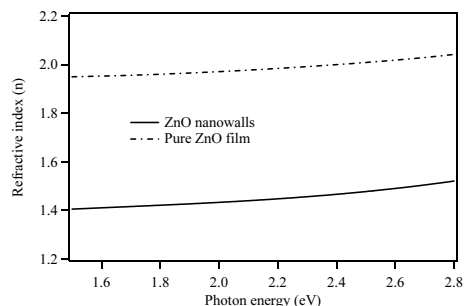


Figure 2 Energy dependent real part of refractive index $n(E)$ for ZnO 3-D nanowall and pure ZnO thin film.

Figure 2 shows the evaluated energy dependent refractive indices $n(E)$ in the narrow energy range of 1.5-2.8 eV. ZnO nanowalls show similar curve shape with that of pure ZnO thin film, but relatively lower refractive indices' values due to the existing of 35% void in the 3-D random walls. By applying the effective medium theory into the SE fitting model, the reasonable refractive indices $n(E)$ were achieved for the void containing sample. We omit $k(E)$ because of approximate zero values in this energy range.

3.3 Depolarization Access to full Mueller matrix allows us to have a complete picture of the sample, and for many cases this is vital for the correct characterisation of a sample. It is well known that the defined depolarization factors P for standard ellipsometer based on simple Mueller matrix expression and P_{gen} for general one based on full Mueller matrix expression are equivalent and less than 1 for an isotropic depolarizing sample. Figure 3 plots energy dependent P and P_{gen} at two different incident angles of 50 and 70 degree. It is observed that the curve of P duplicate completely that of P_{gen} from 1.5-2.8 eV for the designated two incident angles. From above mentioned features of P and P_{gen} , we can discern that isotropic depolarization existing in the 3-D random walls.

When we compare the spectra of P and P_{gen} at 50 degree with those of 70 degree, curves shift can be observed. It reflects the incidental light angle dependence of the ZnO 3-D random walls.

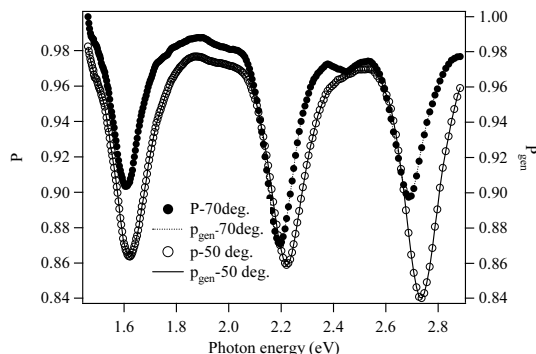


Figure 3 Energy dependent depolarization of ZnO 3-D nanowalls at two different incident angles of 50 and 70 degree.

3.4 Random lasing Room temperature optical characteristics of ZnO nanostructures were studied under optical excitation. Figure 4(a) exhibits the evolution of emission spectra of the ZnO 3-D random-wall nanostructure as a function of pumping laser power. With increasing of the pumping power up to 0.38 MW/cm², multiple laser modes with strong coherent feedback at the wavelengths between 375 and 395 nm were detected. Below 0.38 MW/cm², only amplified broad spontaneous emission (ASE) (373-400 nm) was observed. Consequently, coherent random lasing is resulted by the formation of closed-loop of scattered light inside the ZnO 3-D nanowalls. The relatively lower pump threshold of ZnO 3-D random-wall structure compared to ZnO nanorods arrays embedded in ZnO epilayers (0.8MW/cm²) [16] and ZnO thin film waveguide (0.69 MW/cm²) [23] was due to the high crystal quality of the grown nano-walls. From both our experimental results and reported reference [24], the crystal quality of the sample which determines the band edge emission, scattering length, gain length, and sample size are considered to be responsible for the threshold of the random lasing.

A polarizer in the direction parallel [transverse magnetic (TM)] and perpendicular [transverse electric (TE)] to the 3-D nanowall structure surface was also used to analyze the polarization properties of the lasing light. Figure 4(b) plots the emission spectra of TE and TM modes at various pumping laser powers. Both TE and TM modes show the same pumping power dependent trend and same threshold value, while the lasing intensity of TM mode is weaker than that of TE mode. The reason can attribute to the morphology characteristic of the designated 3-D nanowall structure as reflected by SEM images. The growth orientation of ZnO nanowalls causes the closed-loops, which served as laser cavities, are easily formed in TE direction, thus leading to scattering strength of light is stronger for TE mode. This result is well agreed with isotropic depolarization feature obtained from full Mueller

matrix analysis. Experimentally, it is demonstrated that coherent random lasing is achieved from both TE and TM directions as shown in Fig. 4(b) although their power intensities are a subtly different.

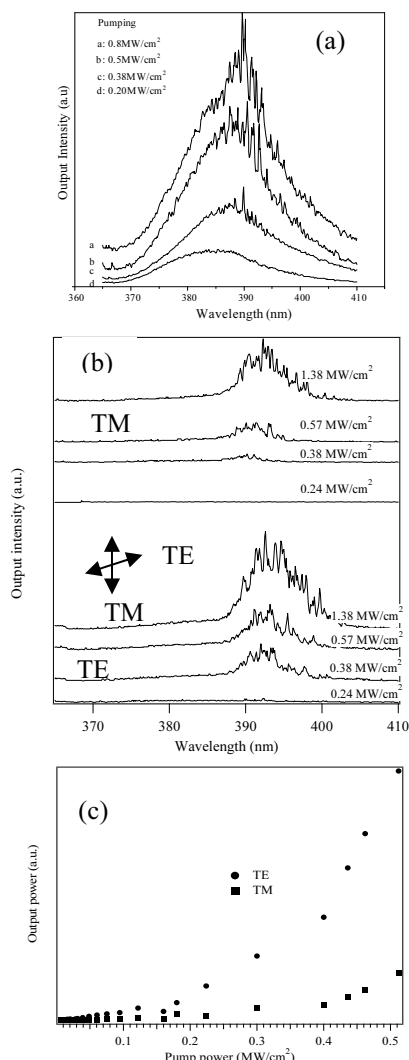


Figure 4 (a) Emission spectra of 3-D ZnO nanowalls at different pumping power; (b) emission spectra of TE and TM modes and (c) the corresponding pumping power dependent emission intensity for TE and TM modes.

4 Conclusions ZnO 3-D random-wall nanostructures have been achieved by a simple thermal chemical reaction/vapour transportation method. Room temperature random lasing was observed at relatively lower threshold 0.38 MW/cm². Compared with TE mode, TM lasing showed weaker intensity but same threshold, which reflects by the structure feature of the 3-D random walls. MMSE analysis reveals the isotropic depolarization characteristics of the 3-D random-walls. As a result, UV lasing at the wide energy range of 375–395 nm with isotropic depolarization state has been successfully achieved in the prepared ZnO nano-random-wall on Si substrate.

Acknowledgements This work is supported in part by the funds from the “A Research for Promoting Technological Seeds” by JST, Japan.

References

- [1] R. F. Service, *Science* **276**, 895 (1997).
- [2] X. Y. Kong and Z. L. Wang, *Nano Lett.* **3**, 1625 (2003).
- [3] W. L. Hughes and Z. L. Wang, *J. Am. Chem. Soc.* **126**, 6703 (2004).
- [4] Z. L. Wang, X. Y. Kong, and J. M. Zuo, *Phys. Rev. Lett.* **91**, 185502 (2003).
- [5] V. S. Letokhov, *Nature* **305**, 103 (1983).
- [6] I. W. Boyd and J. I. B. Wilson, *Nature* **303**, 481 (1983).
- [7] I. Diamond, A. F. McDonagh, C. B. Wilson, S. G. Granelli, S. Nielsen, and R. Jaenicke, *Lancet* **300**, 1175 (1972).
- [8] G. R. Prout, C. W. Lin, R. Benson, U. O. Nseyo, J. J. Daly, P. P. Griffin, J. Kinsey, M. E. Tian, Y. H. Lao, Y. Z. Mian, *N. Engl. J. Med.* **317**, 1251 (1987).
- [9] R. F. Service, *Science* **276**, 895 (1997).
- [10] N. M. Lawandy, R. M. Balachandran, A. S. L. Gomes, and E. Sauvain, *Nature (London)* **368**, 436 (1994).
- [11] D. Wiersma, *Nature (London)* **406**, 132 (2000).
- [12] D. S. Wiersma and S. Cavaliere, *Nature (London)* **414**, 708 (2001).
- [13] H. Cao, Y. G. Zhao, S. T. Ho, E. W. Seelig, Q. H. Wang, and R. P. H. Chang, *Phys. Rev. Lett.* **82**, 2278 (1999).
- [14] H. Cao, J. Y. Xu, D. Z. Zhang, S. H. Chang, S. T. Ho, E. W. Seeling, X. Liu, and R. P. H. Chang, *Phys. Rev. Lett.* **84**, 5584 (2000).
- [15] S. P. Lau, H. Y. Yang, S. F. Yu, C. Y. Yuen, E. S. P. Leong, H. D. Li, and H. H. Hng, *Small* **1**(10), 956 (2005).
- [16] S. F. Yu, Clement Yuen, S. P. Lau, and H. W. Lee, *Appl. Phys. Lett.* **84**(17), 3244 (2004).
- [17] C. Yuen, S. F. Yu, S. P. Lau, and G. C. K. Chen, *J. Cryst. Growth* **287**, 204 (2006).
- [18] S. P. Lau, H. Y. Yang, S. F. Yu, H. L. Li, M. Tanemura, T. Okita, H. Hatano, and H. H. Hng, *Appl. Phys. Lett.* **87**, 013104 (2005).
- [19] L. Miao, S. Tanemura, Y. Ieda, M. Tanemura, Y. Hayashi, H. Y. Yang, S. P. Lau, B. K. Tay, and Y. G. Cao, *Surf. Sci.* **601**, 2660 (2007).
- [20] L. Miao, S. Tanemura, H. Y. Yang, and S. P. Lau, *J. Nanotechnol.* (2009) (in press)
- [21] A. R. Forouhi and I. Bloomer, *Phys. Rev. B* **34**, 7081, (1986).
- [22] A. R. Forouhi and I. Bloomer, *Phys. Rev. B* **38**, 1865 (1988).
- [23] C. Yuen, S. F. Yu, Eunice S. P. Leong, H. Y. Yang, S. P. Lau, and N. S. Chen, *Appl. Phys. Lett.* **86**, 031112 (2005).
- [24] H. Cao, J. Y. Xu, A. L. Burin, E. W. Seeling, X. Liu, and R. P. H. Chang, *IEEE J. Sel. Top. Quantum Electron.* **9**(1), 111 (2003).